Behavior of Damaged Lightweight reinforced Concrete Wide Beams with Near Surface Mounted GFRP Bars under Monotonic and Repeated Loadings

Tamara Alaa Khalaf
Department of Civil Engineering, College of Engineering, Al-Nahrain University, Baghdad, Iraq
tamara.mciv22@ced.nahrainuniv.edu.iq (corresponding author)

Ibrahim S. I. Harba
Department of Civil Engineering, College of Engineering, Al-Nahrain University, Baghdad, Iraq
ibrahim.s.ibrahim@nahrainuniv.edu.iq

Received: 5 April 2025 | Revised: 21 April 2025 and 28 April 2025 | Accepted: 4 May 2025

 DOI: https://doi.org/10.48084/etasr.11303

ABSTRACT

This study investigates the use of Near Surface Mounted (NSM) Glass Fiber Reinforced Polymer (GFRP) bar strengthening and their contribution to flexural strength for damaged lightweight Reinforced Concrete (RC) wide beams under monotonic and repeated loads. The experimental program consists of casting and testing twenty RC wide beams, including two reference wide beams without any GFRP strengthening and eighteen strengthened wide beams. The twenty beams were divided into two main groups, monotonic and repeated loading. The primary variables which have been chosen include the percentage of damage (0%, 50%, and 65%) from the ultimate load of reference beam, the number of GFRP bars, and the reinforcement ratio of GFRP bars. The results indicate that, all strengthened beams have greater ultimate strength than the reference un-strengthened beam in repeated loads, where the increase ranged from 23.8% to 68% for the beam with a damage percent of 65% and 2 Ø12 mm GFRP bars and the beam with a damage percent of 0% and 3 Ø16 mm GFRP bars, respectively, concerning the reference un-strengthened beam. The ratio of repeated ultimate load to monotonic ultimate load ranged from 0.91 to 0.95. The findings indicate that the ultimate load capacity of lightweight wide beam specimens under repeated loading was lower than that observed under monotonic loading. This discrepancy may be attributed to concrete deterioration, which occurs because of the development of internal cracks in the concrete throughout the loading and unloading process. Furthermore, the bond between concrete and steel deteriorates more significantly under repeated stress due to increased dissociation.

Keywords- GFRP bars; near surface mounting; damaged beam; lightweight concrete; damaged wide beam

I. INTRODUCTION

The use of FRP composites in RC components is one of the most promising technologies that address the rehabilitation of infrastructures. GFRP reinforcement has a wide range of applications, including both new construction and building rehabilitation [1, 2]. GFRP composites are revolutionizing the construction industry by offering innovative and sustainable solutions, and are employed in structural elements, such as bars, grids, and profiles. Steel rebars in concrete construction are substituted by GFRP rods. The principal benefits of GFRP are: corrosion-resistance, yielding lasting constructions, exhibiting high strength—approximately more than double the tensile strength of steel—resistance to chemical assaults [3, 4]. Adding GFRP bars enhances the ductility and ultimate load of RC slabs [5]. One of the numerous benefits of lightweight concrete over conventional concrete is its low density, which lowers the dead load [6, 7]. Wide beam, narrow beam, and banded beam are almost synonymous words for beams characterized by limited depth and substantial breadth. They are frequently integrated into ribbed slabs to enhance the formwork. The role of web reinforcement in enhancing the shear capacity of this beam type remains ambiguous, and all design rules have overlooked this factor [8]. Wide beam design has many benefits, including cheaper formwork expenses, thinner floor slabs, and shorter story heights overall [9]. Numerous global design standards for the structural application of concrete, such as ACI 318-14 [10] and Eurocode 8 [11], stipulate the beam width of wide beam-column systems to mitigate the shear lag effect on the development of full-width plastic hinges and to attain the anticipated capacity of wide beams.

Authors in [12] conducted an investigation on the repeated loading performance of flexural bond in GFRP reinforcing bars. The flexural bonding tests utilizing GFRP reinforcing bars were performed in compliance with the criteria stated in BS EN 12269-1 (2000). The bond test comprised three loading schemes: static, monotonic, and variable-amplitude loading, employed to simulate ambient loading conditions. The bond length recorded in the static test was 225 mm, but ACI 440 1R-03 indicated it should be 317 mm. As the link lengthens, the stress on each rib diminishes, resulting in an enhancement of the bonding force. This energy-based analysis may yield an ideal bond length for the specified scenario. At pullout failure after 2,000,000 cycles in the monotonic loading test, the bond strengths were 10.4 MPa and 6.5 MPa, representing 63-70% of the values recorded in the static loading test. The variable loading test indicated that the linear cumulative damage theory used to GFRP bonding may not be appropriate for precisely determining the fatigue limit under variable-amplitude loading circumstances. Authors in [13] conducted an examination of the flexural characteristics of RC beams strengthened with NSM GFRP bars. This study included bending the ends of the NSM GFRP bars in order to postpone or avoid the debonding of NSM FRP and the separation of the concrete cover. This technique effectively increased the load bearing capability of the strengthened beams. The inclined angles of GFRP bars having bent ends were 90 and 45 degrees. Moreover, straight GFRP bars of various lengths were employed for comparative analysis. The test findings indicated that the GFRP bars with curved ends effectively prevented the separation of the concrete cover and enhanced the load-bearing capacity of the reinforced beams.

Authors in [14] provided a comprehensive overview of the progression of damage in concrete beams that are reinforced with GFRP bars. On the whole, the failure mechanism and load–deflection response anticipated by the FE analysis matched well with the actual results across all phases of flexural loading. In addition, the verified Finite Element (FE) model was expanded to include other beam configurations. These configurations were utilized to examine the impact of various bar types and different ratios of GFRP reinforcement on the energy dissipation of concrete beams. This analysis aimed to provide additional insights beyond the constraints of the limited experimental data. The study concludes that the advanced FE model is well-suited as a practical and cost-effective method, particularly for design-focused parametric studies, to accurately simulate and analyze the damage behavior of concrete beams reinforced with GFRP bars. Authors in [15] conducted a test on nine RC rectangular beams that were reinforced using Side Near-Surface Mounted (SNSM). The beams were subjected to four-point bending stresses until they failed. The primary objective of this research is to enhance the structural capability of the RC beams by altering the quantity of strengthening reinforcement and bonding length. The experimental test findings demonstrated that the flexural responses of the specimens were greatly improved when strengthened with SNSM GFRP bars, in comparison to the control specimen. The SNSM approach significantly improved the initial cracking and ultimate loads, energy absorption capabilities, ductility, and stiffness. Furthermore, it has been shown that the length of the link between the reinforced materials has a significant impact on the ability to absorb energy, flexibility, and rigidity. The impact of the bond length on these qualities is more substantial in comparison to the degree of strengthening reinforcement. Authors in [16] conducted a study in which nine beams were reinforced using GFRP bars, whereas one beam was strengthened with steel rebars. The beams were constructed using High-Strength Lightweight Aggregate Concrete (HSLC). The study aimed to investigate the flexural strength and serviceability performance of the beams. Various steel fiber contents, reinforcing ratios, and bar diameters were employed in the testing procedure. The test results revealed that the samples with steel fibers exhibited less deflection and enhanced load-bearing capacity. The experimental measurements of ultimate strengths, midspan deflections, and crack widths were utilized to assess the accuracy of the predictive equations outlined in the standards of the United States, China, and Canada. The rational deflection models for GFRP-reinforced normal weight concrete beams were formulated utilizing data from the current literature. The models were modified by integrating two correction factors: 0.85 for GFRP-reinforced Lightweight Aggregate Concrete (LWAC) beams and 1.35 for steel fiber reinforced LWAC beams.

Authors in [17] conducted experimental and numerical investigations to examine the influence of concrete cover and the area of primary steel reinforcement on the flexural performance of RC beams enhanced with NSM GFRP bars of differing lengths. A total of nine beams, organized into three primary groups, underwent testing using a four-point bending method. The numerical work was conducted using the ANSYS program, a commercial software that employs three-dimensional Finite Element Analysis (FEA). The experimental findings demonstrated that reducing the thickness of the concrete layer resulted in an increase in the bending strength of the RC beams. However, this enhancement was no longer seen when the length of the NSM GFRP bars was decreased. The numerical findings exhibited agreement with the experimental results. Authors in [18] examined the static and dynamic behavior of RC beams, both with and without reinforcement. The non-destructive vibration tests were used to evaluate the reaction of RC beams at various levels of concrete damage. Additionally, an analysis was conducted on the damage of an RC beam using bending and vibration testing, without any reinforcement. Subsequently, the beam model with an NSM GFRP rod was evaluated using the same loading conditions. The following experimental findings are presented and analyzed, specifically focusing on the variations in frequency values that correspond to the progression of damage in RC beams reinforced with NSM Carbon Fiber Reinforced Polymer (CFRP) and GFRP rods. Authors in [19] conducted a comprehensive analysis of the bonding characteristics between GFRP bars and concrete. The study involved analyzing the impact of many parameters, including bar length, diameter, concrete strength, concrete cover thickness, and rebar surface morphology. This study was conducted using a series of pull-out tests. The test results indicate that the bond strength of GFRP bars is mostly influenced by their surface morphology, embedment length, and diameter. The impact of concrete

strength and cover thickness on the bonding strengths of GFRP rebars to concrete appears to be negligible. The results indicate that ribbed GFRP bars exhibit a maximum bonding energy of 89.4 N.mm and a mean bond strength of 11.9 MPa.

The present study aims to provide new insights into the use of NSM GFRP bar strengthening and its contribution to the flexural strength of damaged lightweight RC wide beams under both monotonic and repeated loading conditions.

II. EXPERIMENTAL PROGRAM

The experimental work involves the production and testing of PΨ wide beams, comprising two reference beams without any GFRP reinforcement and 18 beams with reinforcement. The beams were divided into two main groups: the first group was tested under monotonic loading, while the second group was subjected to repeated loading. The NSM method was used to strengthen the beams with GFRP bars. The primary variables selected for this study include the percentage of damage (0%, 50%, and 65%) relative to the ultimate load of the reference beam, the number of GFRP bars, and the reinforcement ratio of the GFRP bars. All tested beams before strengthening had the same length, width, height, reinforcement and they were subjected to two-point loads, as shown in Figure 1.

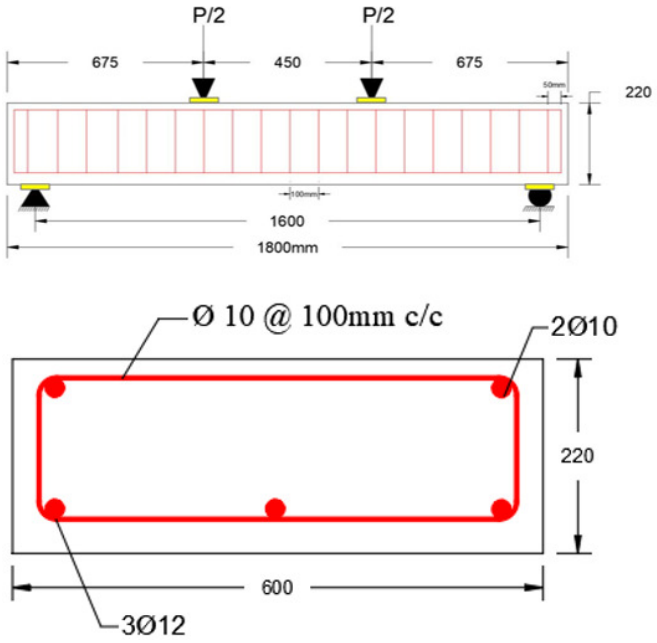

Fig. 1. Details of control (un-strengthened) wide beams.

Figure 2 presents the details of the strengthened beams. The concrete cover for the bottom face of the beam = 40 mm and the other sides = 25 mm. All 18 beams after the damage were strengthened with two or three GFRP bars with a diameter of 12 mm or 16 mm using the NSM technique glued inside the cover of the bottom face of the wide beam (4 cm). Precautions were taken to avoid local failure at loading point and supports by means of steel plates. The stirrups of all beams have a diameter of 10 mm with a spacing of 100 mm. Table I outlines the details of the tested wide beams. The letter "W" denotes a wide beam, while the subsequent symbols "M" or "R" indicate whether the specimen was tested under monotonic or repeated loading, respectively. The next digit numbers after the symbols show the damage percentage, number of GFRP bars, and diameter of GFRP bars, respectively. The percentage of damage (0%, 50%, and 65%) of the ultimate load of the reference beam was chosen to get the damaged (pre-load) LWRCW beams. The beams were loaded to the load according to the selected damage percentages from the ultimate load of the reference beam. All beams cracked at the end of this required damage stage. Then monotonic loading was applied until failure occurred.

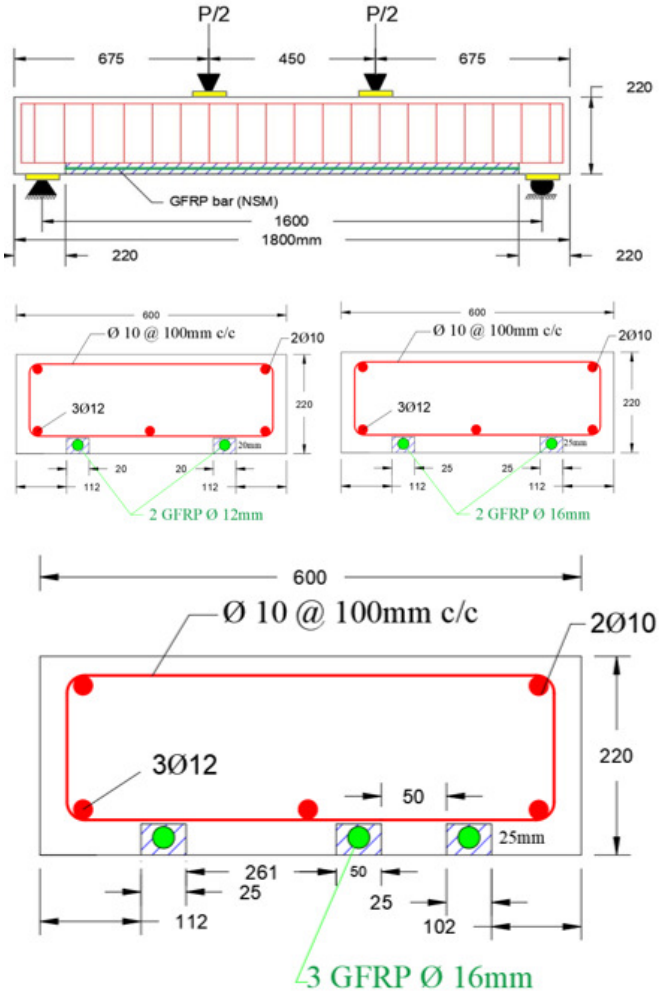

Fig. 2. Details of strengthened wide beams.

Table II presents the tensile properties of the steel reinforcing rebars used in the study, while Table III shows the results of the tensile test for GFRP bars. Figure 3 portrays the LECA particles used in this paper. Table IV displays the properties of LECA.

TABLE I. TESTED BEAMS DETAILS

Group ID	Load type	Beam ID	Percentage of damage relative to the ultimate load of the control beam (%)	No. of GFRP bars	Diameter of GFRP bars (mm)
1	Mon. loads	WM0-CB	Reference	-	-
		WM0-2-12	0	2	12
		WM50-2-12	50	2	12
		WM65-2-12	65	2	12
		WM0-2-16	0	2	16
		WM50-2-16	50	2	16
		WM65-2-16	65	2	16
		WM0-3-16	0	3	16
		WM50-3-16	50	3	16
		WM65-3-16	65	3	16
2	Rep. loads	WR0-CB	Reference	-	-
		WR0-2-12	0	2	12
		WR50-2-12	50	2	12
		WR65-2-12	65	2	12
		WR0-2-16	0	2	16
		WR50-2-16	50	2	16
		WR65-2-16	65	2	16
		WR0-3-16	0	3	16
		WR50-3-16	50	3	16
		WR65-3-16	65	3	16

TABLE II. TENSILE CHARACTERISTICS OF THE EMPLOYED STEEL REINFORCING REBARS

Nominal diameter (mm)	Nominal area (mm^2)	Average of yield tensile stresses, f_y (MPa)	Average of ultimate tensile strengths, f_u (MPa)	Elongation due to ultimate stress (%)
10	78.6	590	762	14.5
12	113	605	779	12

TABLE III. RESULTS OF TENSILE TEST FOR GFRP BARS.

Diameter (mm)	Initial area (mm^2)	Modulus of elasticity (MPa)	Tensile strength (MPa)	Weight (g/m)
12.6	126.7	46000*	758*	281.3
16	197.9	46000*	724*	427.1

Source: From the product PDF of the manufacturer

TABLE IV. PROPERTIES OF LECA

Declared performance		
Essential characteristics	Performance	
Particle shape	Semi-round / cracked	
Aggregate size	0-8 mm	
	Passing	
Aggregate size distribution (Dry sieving) (ASTM C136-06)	Sieves (mm)	Typical
	25.4	100%
	19.05	100%
	12.7	100%
	9.5	90%
	4.75	42%
	2.36	13%
	1.18	7%
	0.3	0-1%
	0.15	0-0.5%
Loose bulk density (ASTM C29-97)	Limits: 600 kg/m^3	
	Typical: 700 kg/m^3	

Fig. 3. LECA particles used in the experimental program.

Table V shows the details of the concrete mix proportion. Figure 4 illustrates the installation of reinforcement and the pouring of concrete for beams. Figure 5 depicts the Strengthening method using GFRP bars.

TABLE V. DETAILS OF LWAC PROPORTION

Cement	Sand	LECA	Water
500	755	470	190

Fig. 4. Installation of reinforcement mesh concrete pouring.

Fig. 5. Strengthening using GFRP bars.

III. EXPERIMENTAL RESULTS

A. *Hardened Concrete Properties*

Table VI shows the properties of hardened LWAC.

TABLE VI. PROPERTIES OF HARDENED LWAC

Compressive strength (cubes) (MPa)	Compressive strength (cylinders) (MPa)	Splitting tensile strength (MPa)	Modulus of rupture (MPa)	Oven dry density (kg/m^3)
40.52	33.1	3.29	3.83	1820

B. *Initial Crack Loads at Monotonic Loading*

Table VI presents the findings from experiments related to cracking loads, deflections, and failure loads. The first flexural fracture was seen at varying applied loads (36-45 kN) across all samples, with a P_{cr}/P_u percentage ranging from 20% to 34.2%, as illustrated in Table VII. It was established that an increase in the added area of GFRP bars had a minimal impact on the P_{cr}/P_u percentage, and a rise in the percentage of damage also had a negligible influence on the P_{cr}/P_u percentage. This is because the initial cracking load depends mainly on concrete properties.

TABLE VII. RESULTS OF THE TESTED WIDE BEAMS UNDER MONOTONIC LOADS

Beam ID	Damage (%)	Cracking Load (kN)	Ultimate load (Pu) (kN)	Beam ID	Damage (%)
WM0-CB	-	44	128.16	8	34.2
WM0-2-12	-	44	199.7	20.76	22
WM0-2-16	-	43	210.1	17.64	20.5
WM0-3-16	-	45	220.2	14.43	20.4
WM50-2-12	50	39*	185.2	21.74	21.1
WM50-2-16	50	44*	199	18.93	22.1
WM50-3-16	50	43*	209.3	15.69	20.5
WM65-2-12	65	36*	163.9	18.93	22
WM65-2-16	65	36*	180.3	19.8	20
WM65-3-16	65	40*	190.2	18.78	21

C. *Load – Mid Span Deflection Under Monotonic Loading*

Figures 6 and 7 illustrate the correlation between the applied load and mid-span deflection, ranging from zero load to the failure stage for all tested beams. All tested beams initially exhibited linear deflection. Subsequent to the cracking load, the examined beams exhibited semi-linear deflection with increasing load; however, the slope of the deflection lines was reduced compared to the pre-cracking phase, and the deflection curves diverged according to the extent of cracking and the degree of stiffness degradation. The slope of this linear segment differed across specimens within the same group. As loads approached the ultimate load, tested beams exhibited nonlinear deflection in relation to the applied load.

D. *Load-carrying Capacity and Failure Mode at Monotonic Loads*

In the reference beam (WM0-CB), the failure was flexural, while, in the rest of the strengthened beams, shear-flexural failure occurred. Table VIII shows that the ultimate strength of all strengthened beams is higher than that of the reference beam. The increase in ultimate strength ranged from 27.9% to 71.8% for the beam with a damage percentage of 65% and 2 Ø12 mm GFRP bars, and for the beam with a damage percentage of 0% and 3 Ø16 mm GFRP bars, respectively, in comparison to the reference un-strengthened beam. Table IX demonstrates the effect of damage percentage on the ultimate loads of the tested wide beams under monotonic loads. The cracking pattern at failure for monotonic specimens is shown in Figures 8-16.

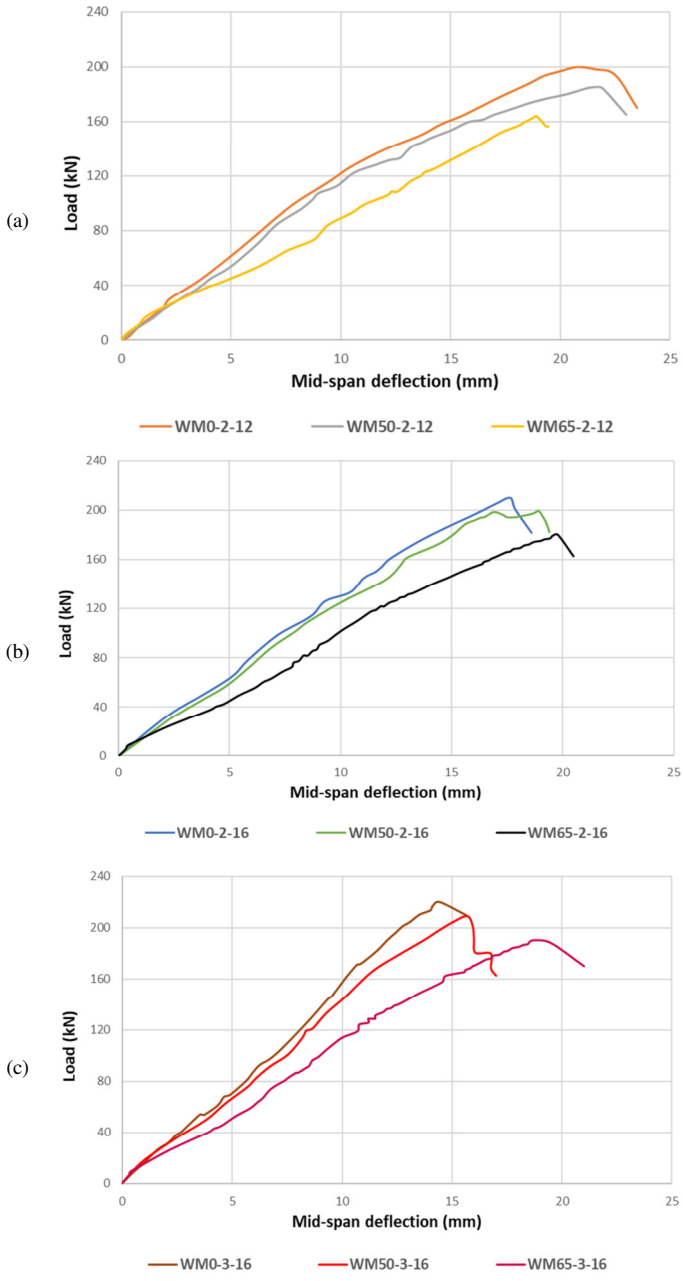

Fig. 6. Effect of percentage of damage on load–deflection curves: (a) group with 2 Ø12 mm GFRP bars, (b) group with 2 Ø16 GFRP bars, (c) group with 3 Ø16 mm GFRP bars.

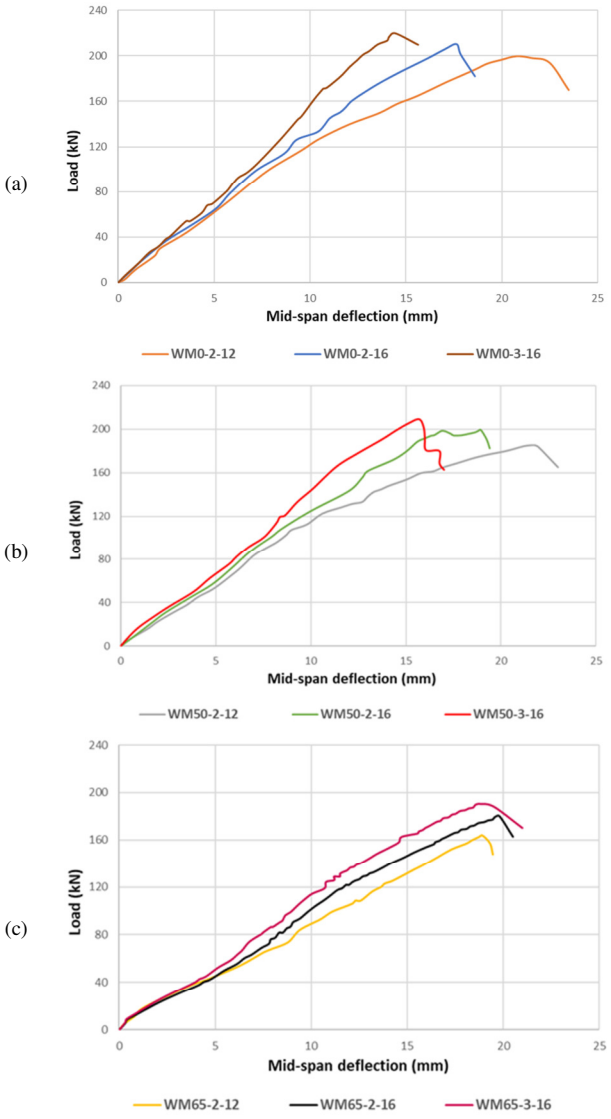

Fig. 7. Effect of percentage of added GFRP bar area on load–deflection curves: (a) group with 0% damage, (b) group with 50% damage, (c) group with 65% damage.

TABLE VIII. STRENGTHENING EFFECT ON THE ULTIMATE LOAD OF THE TESTED WIDE BEAMS

Beam ID	Damage ratio %	Ultimate load (P_u) (kN)	P_u increment percentage with respect to control beam (%)	P_u increment percentage with respect to the reference beam of each group (%)
WM0-CB	-	128.16	Ref.	-
WM0-2-12	-	199.7	55.8	Ref.
WM0-2-16	-	210.1	63.9	5.2
WM0-3-16	-	220.2	71.8	10.3
WM50-2-12	50	185.2	44.5	Ref.
WM50-2-16	50	199.0	55.2	7.5
WM50-3-16	50	209.3	63.3	13
WM65-2-12	65	163.9	27.9	Ref.
WM65-2-16	65	180.3	40.7	10
WM65-3-16	65	190.2	48.4	16

TABLE IX. EFFECT OF DAMAGE PRESENTAGE ON THE ULTIMATE LOADS OF THE TESTED WIDE BEAMS UNDER MONOTONIC LOADS

Beam ID	Damage ratio %	Ultimate load (P_u) (kN)	P_u decrement percentage with respect to the un-damaged beam of each group (%)
WM0-2-12	-	199.7	Ref.
WM50-2-12	50	185.2	7.3
WM65-2-12	65	163.9	17.9
WM0-2-16	-	210.1	Ref.
WM50-2-16	50	199.0	5.3
WM65-2-16	65	180.3	14.2
WM0-3-16	-	220.2	Ref.
WM50-3-16	50	209.3	5.0
WM65-3-16	65	190.2	13.6

Fig. 8. Final crack pattern of specimen WM0-CB.

Fig. 9. Final crack pattern of specimen WM0-2-12.

Fig. 10. Final crack pattern of specimen WM0-2-16.

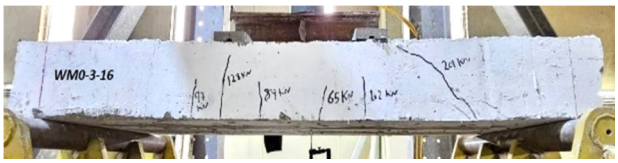

Fig. 11. Final crack pattern of specimen WM0-3-16.

Fig. 12. Final crack pattern of specimen WM50-2-12.

Fig. 13. Final crack pattern of specimen WM50-2-16.

Fig. 14. Final crack pattern of specimen WM50-3-16.

Fig. 15. Final crack pattern of specimen WM65-2-12.

Fig. 16. Final crack pattern of specimen WM65-2-16.

Fig. 17. Final cracks pattern of specimen WM65-3-16.

E. Initial Crack Loads at Repeated Loads

Table X presents the findings from experiments related to cracking loads, deflections, and failure loads. The first flexural fracture manifested at varying applied loads (31-42 kN) across all specimens, with P_{cr}/P_u percentages ranging from around 17.5% to 30.3%, which is marginally lower than observed under monotonic loading conditions. It was found that an increase in the increased area of GFRP bars had a minimal impact on the P_{cr}/P_u percentage, and a rise in the percentage of damage also had a negligible influence on the P_{cr}/P_u percentage, in case or repeated load.

TABLE X. RESULTS OF THE TESTED WIDE BEAMS UNDER REPEATED LOADS

Beam ID	Damage (%)	P_{cr} (kN)	P_u (kN)	Deflection at P_u (mm)	P_{cr}/P_u	No. of cycles at P_u
WR0-CB	-	37	122.1	9.1	30.3	18
WR0-2-12	-	39	181.7	21.6	21.4	20
WR0-2-16	-	41	193.1	19.3	21.2	20
WR0-3-16	-	42	205.1	15.9	20.4	18
WR50-2-12	50	37*	175	21.9	21.1	19
WR50-2-16	50	38*	190.61	20.4	19.9	18
WR50-3-16	50	37*	198.8	19.3	18.6	17
WR65-2-12	65	38*	151.1	21.2	25.1	19
WR65-2-16	65	39*	166.8	22.3	23.4	18
WR65-3-16	65	31*	177.4	20.6	17.5	18
*First cracked load happened at the first stage (damage) loading.						

F. Load – Mid Span Deflection under Repeated Loading

Ten wide beams were tested under repeated load using displacement control. The applied load protocol according to FEMA [20]. The initial phase of low cycle fatigue in the applied load regimen involved conducting ten cycles of deformation amplitude. Figure 18 illustrates a comparison of the relationships between applied monotonic load and mid-span deflection, ranging from zero loadings to the failure stage, alongside the connections between applied repetitive load and mid-span deflection within the same parameters for all tested beams.

(a)

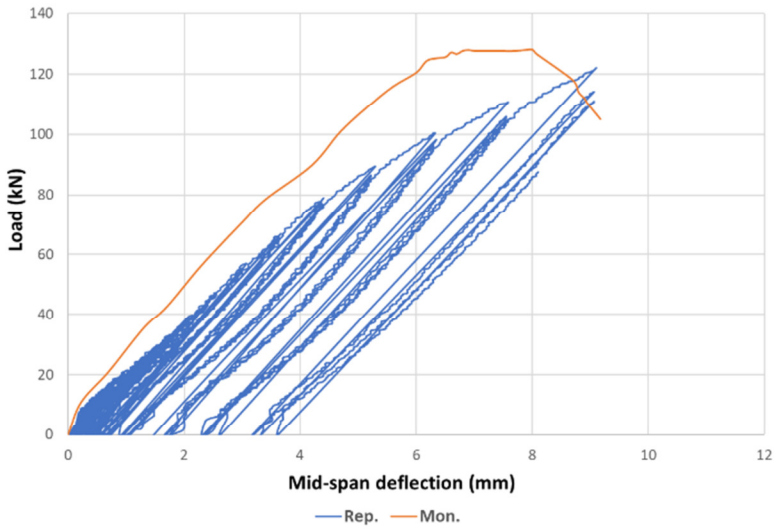

(b)

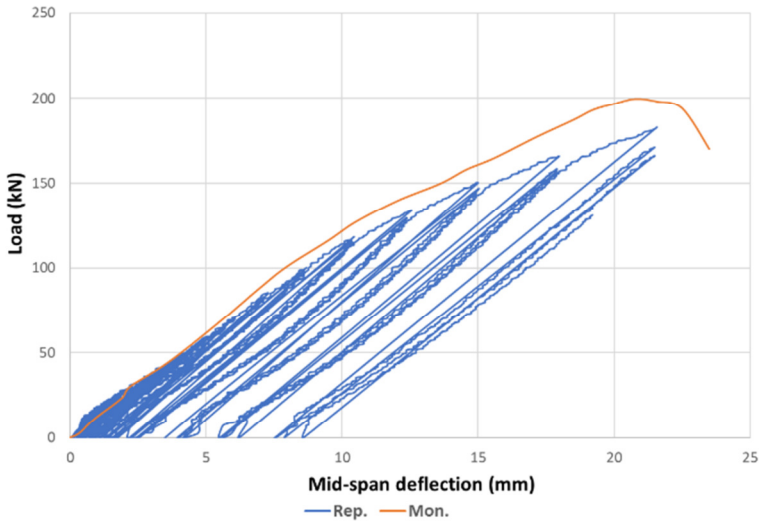
Load (kN)
Mid-span deflection (mm)
Rep.
Mon.

(c)

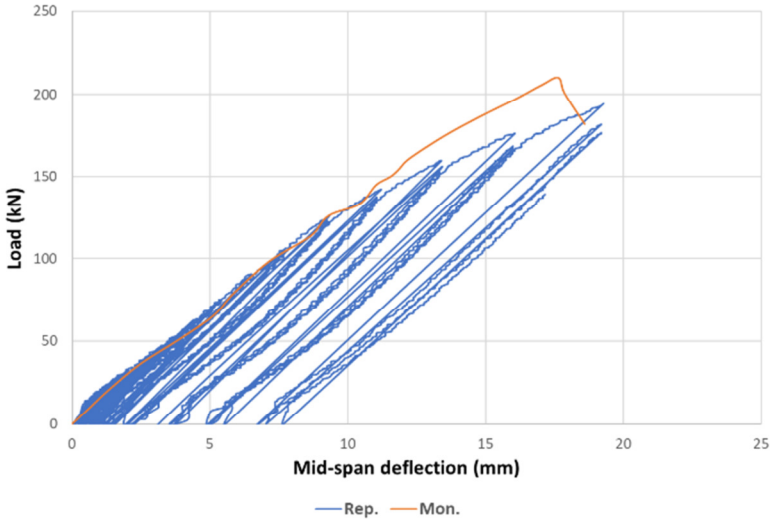
Load (kN)
Mid-span deflection (mm)
Rep.
Mon.

(d)

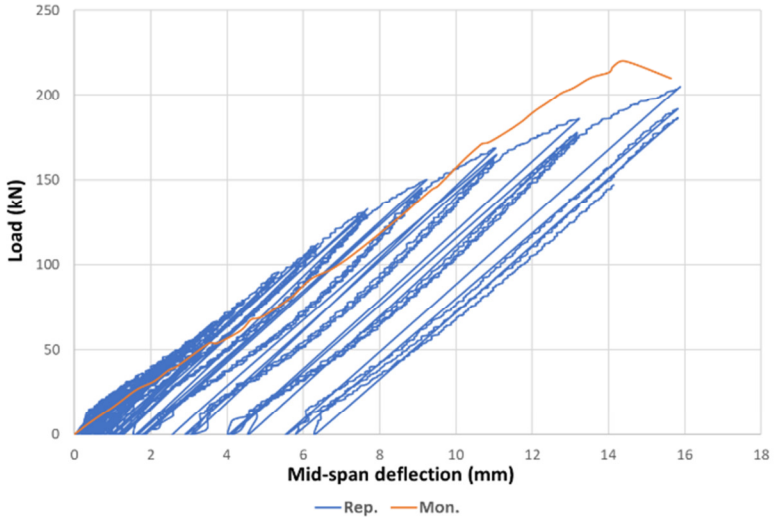
Load (kN)
Mid-span deflection (mm)
Rep.
Mon.

(e)

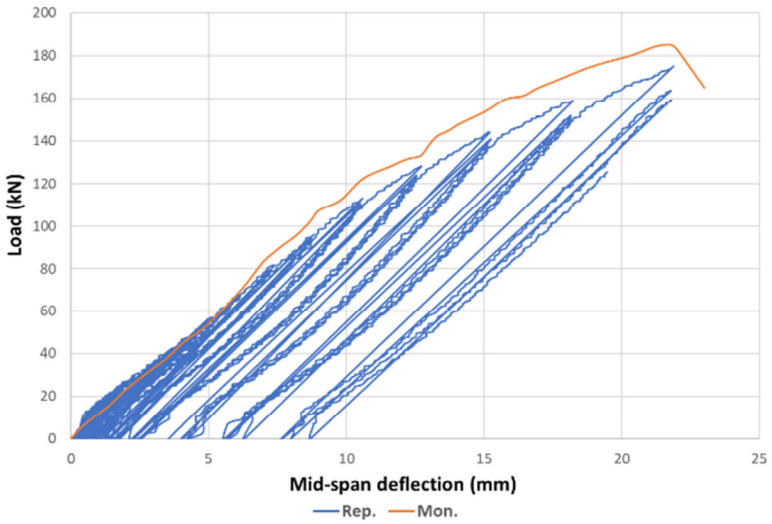
Load (kN)
Mid-span deflection (mm)
Rep.
Mon.

(f)

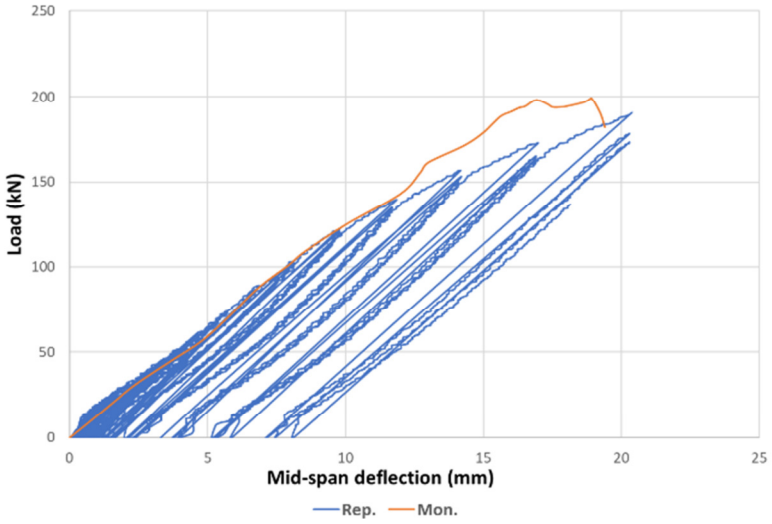
Load (kN)
Mid-span deflection (mm)
Rep.
Mon.

(g)

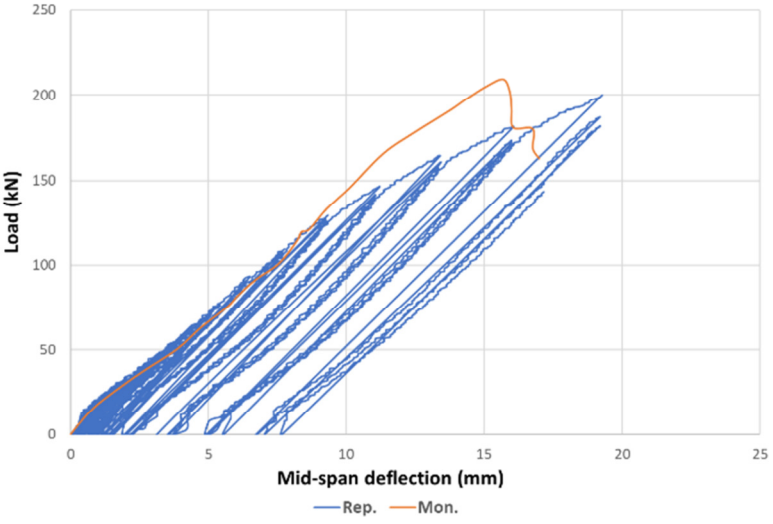
Load (kN)
Mid-span deflection (mm)
Rep.
Mon.

(h)

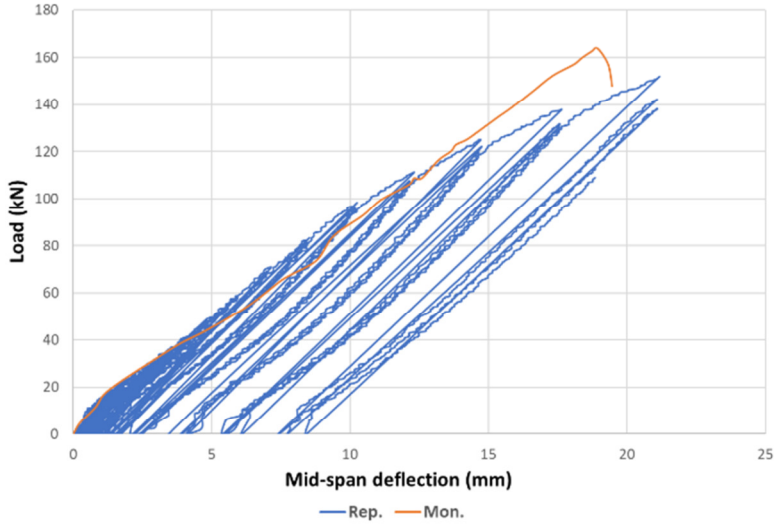

(i)

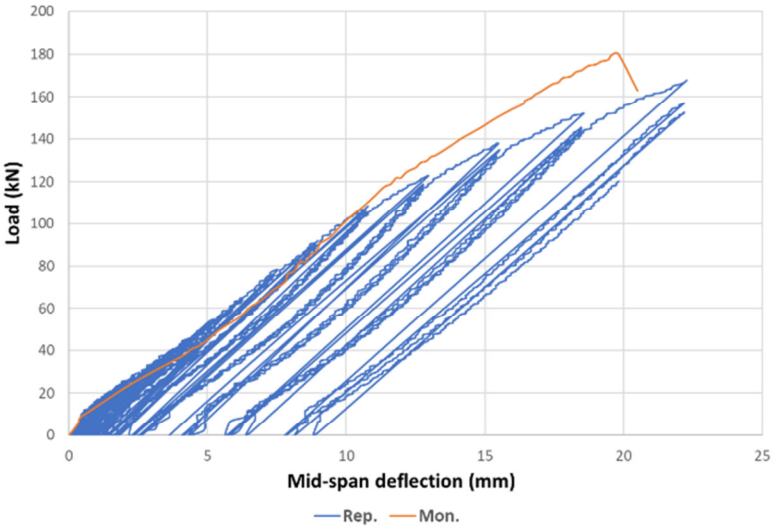

(j)

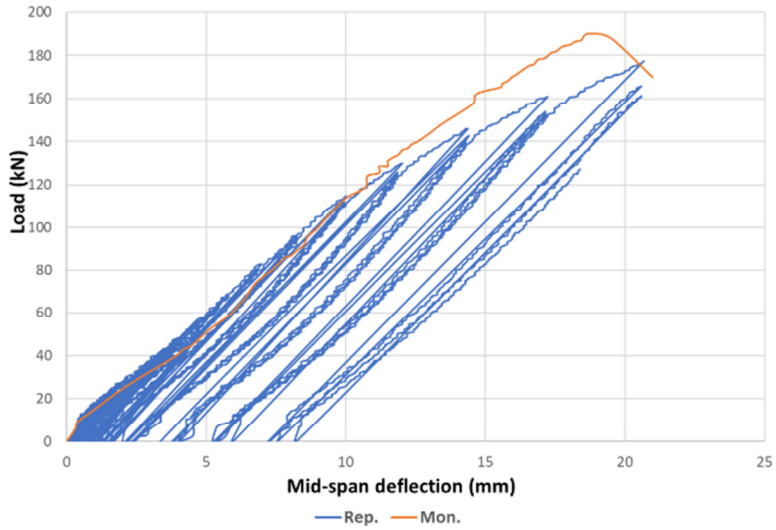

Fig. 18. Continued comparison between repeated and monotonic test on load-deflection behavior at mid-span: (a) WR0-CB, (b) WR0-2-12, (c) WR0-2-16, (d) WR0-3-16, (e) WR50-2-12, (f) WR50-2-16, (g) WR50-3-16, (h) WR65-2-12, (i) WR65-2-16, (j) WR65-3-16.

Table XI summarizes the relevant mid-span deflection and ultimate applied repeated load for all beams. A significant difference is evidenced in the behavior of the beams subjected to monotonic versus repetitive loads near the ultimate stage. The results indicate that the stiffness of lightweight wide beam specimens under repeated loads was inferior to that under monotonic loads. This discrepancy can be attributed to concrete deterioration, which occurs owing to the increase in the number of internal cracks in concrete during the process of loading and unloading. Additionally, the bonding between the concrete and steel experiences greater separation due to the repeated load effect.

TABLE XI. LOAD AND THE CORRESPONDING DEFLECTION FOR BEAMS AT ULTIMATE REPEATED LOADING STAGE

Beam ID	Damage (%)	Ultimate load (P_u) (kN)	Deflection at P_u (mm)
WR0-CB	-	122.1	9.1
WR0-2-12	-	181.7	21.6
WR0-2-16	-	193.1	19.3
WR0-3-16	-	205.1	15.9
WR50-2-12	50	175	21.9
WR50-2-16	50	190.61	20.4
WR50-3-16	50	198.8	19.3
WR65-2-12	65	151.1	21.2
WR65-2-16	65	166.8	22.3
WR65-3-16	65	177.4	20.6

G. Load-carrying Capacity and Failure Mode at Repeated Loads

In the reference beam (WR0-CB), flexural failure occurred, while, in the rest of the strengthened beams, a shear-flexural failure took place. Table XII shows that all strengthened beams have greater ultimate strength than the reference un-strengthened beam, where the increase ranged from 23.8 to 68 % for the beam with a damage percent of 65 % and 2 Ø12 mm GFRP bars and the beam with a damage percent of 0% and 3 Ø16 mm GFRP bars, respectively, concerning the reference un-strengthened beam. Table XIII presents the effect of damage present on the ultimate loads of the tested wide beams under repeated loads, while Table XIV illustrates a comparison in the ultimate loads of the monotonic and repeated load tests.

TABLE XII. EFFECT OF AMOUNT OF STRENGTHENING ON THE ULTIMATE LOADS OF THE TESTED WIDE BEAMS UNDER REPEATED LOADS

Beam ID	Ultimate load P_u (kN)	P_u increment percentage with respect to the control beam (%)	P_u increment percentage with respect to the reference beam of each group (%)
WR0-CB	122.1	Ref.	-
WR0-2-12	181.7	48.8	Ref.
WR0-2-16	193.1	58.1	6.3
WR0-3-16	205.1	68	12.9
WR50-2-12	175	43.3	Ref.
WR50-2-16	190.61	56.1	8.9
WR50-3-16	198.8	62.8	13.6
WR65-2-12	151.1	23.8	Ref.
WR65-2-16	166.8	36.6	10.4
WR65-3-16	177.4	45.3	17.4

TABLE XIII. EFFECT OF DAMAGE PRESENT ON THE ULTIMATE LOADS OF THE TESTED WIDE BEAMS UNDER REPEATED LOADS

Beam ID	Ultimate load P_u (kN)	P_u decrement percentage with respect to the un-damaged beam of each group (%)
WR0-2-12	181.7	Ref.
WR50-2-12	175.0	3.7
WR65-2-12	151.1	16.8
WR0-2-16	193.1	Ref.
WR50-2-16	190.61	1.3
WR65-2-16	166.8	13.6
WR0-3-16	205.1	Ref.
WR50-3-16	198.8	3.1
WR65-3-16	177.4	13.5

TABLE XIV. COMPARISON IN ULTIMATE LOADS OF MONOTONIC AND REPEATED LOAD TEST

Specimens	P_u (kN) under monotonic load (M)	(P_u) (kN) under repeated load (R)	$P_{u(R)}/P_{u(M)}$ (%)
WR0-CB	128.16	122.1	0.95
WR0-2-12	199.7	181.7	0.91
WR0-2-16	210.1	193.1	0.92
WR0-3-16	220.2	205.1	0.93
WR50-2-12	185.2	175.0	0.94
WR50-2-16	199.0	190.61	0.96
WR50-3-16	209.3	198.8	0.95
WR65-2-12	163.9	151.1	0.92
WR65-2-16	180.3	166.8	0.93
WR65-3-16	190.2	177.4	0.932

Figures 19-28 show the crack pattern of specimens under the effect of repeated loads.

Fig. 19. Crack pattern of specimen WR0-CB.

Fig. 20. Crack pattern of specimen WR0-2-12.

Fig. 21. Crack pattern of specimen WR0-2-16.

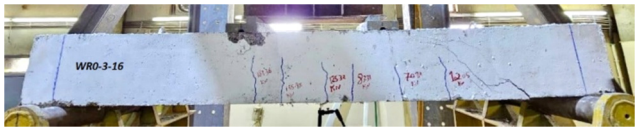

Fig. 22. Crack pattern of specimen WR0-3-16.

Fig. 23. Crack pattern of specimen WR50-2-12.

Fig. 24. Crack pattern of specimen WR50-2-16.

Fig. 25. Crack pattern of specimen WR50-3-16.

Fig. 26. Crack pattern of specimen WR65-2-12.

Fig. 27. Crack pattern of specimen WR65-2-16.

Fig. 28. Crack pattern of specimen WR65-3-16.

IV. CONCLUSION

This study examines the application of Near-Surface Mounted (NSM) Glass Fiber Reinforced Polymer (GFRP) bars for strengthening damaged lightweight Reinforced Concrete (RC) wide beams. It also evaluates their contribution to flexural strength under both monotonic and repeated loads. The following conclusions are drawn from this study.

- The first flexural fracture developed at varying applied loads (36-45 kN) for all specimens, with P_{cr}/P_u percentages ranging from 20% to 34.2%. Augmenting the additional area of GFRP bars exerts a little influence on the P_{cr}/P_u percentage, while an increase in the damage % similarly has a negligible effect on the P_{cr}/P_u percentage.
- All strengthened beams exhibit superior ultimate strength compared to the reference unreinforced beam under monotonic loads, with increases ranging from 27.9% to 71.8% for the beam with 65% damage and 2 Ø12 mm GFRP bars, and the beam with 0% damage and 3 Ø16 mm GFRP bars, respectively, in relation to the reference unreinforced beam.
- Whenever the quantity of supplementary GFRP bars is augmented, the ultimate strength of the beam with 2 Ø16 mm and 3 Ø16 mm GFRP bars is increased by approximately 5.2 and 10.3%, respectively, compared to the beam with 2 Ø12 mm GFRP bars for the un-damaged beams, 7.5 and 13 %, respectively, compared to the beam with 2 Ø12 mm GFRP bars for the 50% damaged beams, and 10 and 16 %, respectively, compared to the beam with 2 Ø12 mm GFRP bars for the 65% damaged beams, in case of monotonic load.
- The first flexural crack occurred at different applied load (31-42 kN) for all specimens, with a P_{cr}/P_u percentage of about 17.5-30.3 %, which is slightly less than in the case of monotonic load. It was concluded that increasing the added area of GFRP bars has a small effect on the P_{cr}/P_u percentage, and increasing the percentage of damage has a small effect on the P_{cr}/P_u percentage, in case of repeated load.
- Each strengthened beam exhibits superior ultimate strength compared to the reference unreinforced beam under repeated loading, with increases ranging from 23.8% to 68%, for the beam with 65% damage and 2 Ø12 mm GFRP bars, and the beam with 0% damage and 3 Ø16 mm GFRP bars, respectively, in relation to the reference unreinforced beam.
- In repeated loads, increasing the area of added GFRP bars results in an enhancement of ultimate strength by about 6.3 and 12.9 % for the beam with 2 Ø16 mm and 3 Ø16 mm GFRP bars, respectively, concerning the beam with 2 Ø12 mm GFRP bars for the un-damaged beams, and 8.9 and 13.6 % for the beam with 2 Ø16 mm and 3 Ø16 mm GFRP bars, respectively, concerning the beam with 2 Ø12 mm GFRP bars for the 50% damaged beams, and 10.4 and 17.4 % for the beam with 2 Ø16 mm and 3 Ø16 mm GFRP bars, respectively, concerning the beam with 2 Ø12 mm GFRP bars for the 65% damaged beams. It is clear that the greater the percentage of damage is, the greater is the effect of the area of added GFRP bars.
- The ratio of repeated ultimate load / monotonic ultimate load was about 0.91 to 0.95. The results indicate that the ultimate load capacity of lightweight wide beam specimens exposed to cyclic loads was inferior to that under monotonic loads. This mismatch may be ascribed to concrete degradation, which transpires due to the proliferation of internal fissures in the concrete throughout the loading and unloading procedure. Moreover, the adhesion between the concrete and steel undergoes increased dissociation as a result of the repetitive loading impact.
- For monotonic or repeated loading, in the case of the reference un-strengthened beam, a flexural failure occurred, while in the rest of the strengthened beams with GFRP bars, a shear-flexural failure took place.

REFERENCES

[1] A. Dasgupta, "Retrofitting of Concrete Structure with Fiber Reinforced Polymer," *International Journal for Innovative Research in Science & Technology*, vol. 4, no. 9, pp. 42–49, Feb. 2018.

[2] B. F. Abdulkareem, A. F. Izzet, and N. Oukaili, "Post-Fire Behavior of Non-Prismatic Beams with Multiple Rectangular Openings Monotonically Loaded," *Engineering, Technology & Applied Science Research*, vol. 11, no. 6, pp. 7763–7769, Dec. 2021, https://doi.org/10.48084/etasr.4488.

[3] M. Abdulkhaliq and A. H. Al-Ahmed, "The Flexural Behavior of One-Way Concrete Bubbled Slabs Reinforced by GFRP-Bars with Embedded Steel I-Sections," *Engineering, Technology & Applied Science Research*, vol. 14, no. 4, pp. 15860–15870, Aug. 2024, https://doi.org/10.48084/etasr.7680.

[4] *Guide for the design and construction of externally bonded FRP systems for strengthening concrete structures*, 440-2R, American Concrete Institute, MI, USA, 2017.

[5] M. R. Rasheed and S. D. Mohammed, "Structural behavior of one-way slabs reinforced by a combination of GFRP and steel bars: An experimental and numerical investigation," *Journal of the Mechanical Behavior of Materials*, vol. 33, no. 1, May 2024, Art. no. 20240002, https://doi.org/10.1515/jmbm-2024-0002.

[6] T. M. Ismael and S. D. Mohammed, "Structural performance of fiber-reinforced lightweight concrete slabs with expanded clay aggregate," *Materials Today: Proceedings*, vol. 42, pp. 2901–2908, 2021, https://doi.org/10.1016/j.matpr.2020.12.746.

[7] R. Rajprakash and A. Krishnamoorthi, "Experimental Study on Light Weight Concrete Using Leca," *International Journal of ChemTech Research*, vol. 10, no. 8, pp. 98–109, 2017.

[8] A. A. Soliman, D. M. Mansour, A. Ebid, and A. H. Khalil, "Shallow and Wide RC Beams, Definition, Capacity and Structural Behavior – Gap Study," *The Open Civil Engineering Journal*, vol. 17, no. 1, Aug. 2023, https://doi.org/10.2174/18741495-v17-e230725-2023-28.

[9] J. M. LaFave and J. K. Wight, "Reinforced Concrete Wide-Beam Construction vs. Conventional Construction: Resistance to Lateral Earthquake Loads," *Earthquake Spectra*, vol. 17, no. 3, pp. 479–505, Aug. 2001, https://doi.org/10.1193/1.1586185.

[10] *Building Code Requirements for Structural Concrete,* ACI CODE-318-19(22), American Concrete Institute, MI, USA, 2022.

[11] *Eurocode 8: Design of structures for earthquake resistance – Part 1: General rules, seismic actions and rules for buildings,* BS EN 1998-1, London, UK, Dec. 2004.

[12] M. Ju and H. Oh, "Experimental Assessment on the Flexural Bonding Performance of Concrete Beam with GFRP Reinforcing Bar under Repeated Loading," *International Journal of Polymer Science*, vol. 2015, pp. 1–11, 2015, https://doi.org/10.1155/2015/367528.

[13] R. M. Reda, I. A. Sharaky, M. Ghanem, M. H. Seleem, and H. E. M. Sallam, "Flexural behavior of RC beams strengthened by NSM GFRP Bars having different end conditions," *Composite Structures*, vol. 147, pp. 131–142, Jul. 2016, https://doi.org/10.1016/j.compstruct. 2016.03.018.

[14] W. Yang, X. He, and L. Dai, "Damage behaviour of concrete beams reinforced with GFRP bars," *Composite Structures*, vol. 161, pp. 173–186, Feb. 2017, https://doi.org/10.1016/j.compstruct.2016.11.041.

[15] Md. A. Hosen, U. J. Alengaram, M. Z. Jumaat, N. H. R. Sulong, and Kh. M. U. Darain, "Glass Fiber Reinforced Polymer (GFRP) Bars for Enhancing the Flexural Performance of RC Beams Using Side-NSM Technique," *Polymers*, vol. 9, no. 5, May 2017, Art. no. 180, https://doi.org/10.3390/polym9050180.

[16] Y. Sun, T. Wu, and X. LIU, "Flexural behavior of steel fiber–reinforced lightweight aggregate concrete beams reinforced with glass fiber–reinforced polymer bars," *Journal of Composites for Construction*, vol. 23, no. 2, 2019, Art. no. 04018081.

[17] Hesham EL-Emam, Alaa El-Sisi, Ramy Reda, Mohamed Bneni, and Mohamed Seleem, "Effect of concrete cover thickness and main reinforcement ratio on flexural behavior of RC beams strengthened by NSM-GFRP bars," *Frattura ed Integrità Strutturale*, vol. 14, no. 52, pp. 197–210, Mar. 2020, https://doi.org/10.3221/IGF-ESIS.52.16.

[18] R. Capozucca, E. Magagnini, M. V. Vecchietti, and S. Khatir, "RC beams damaged by cracking and strengthened with NSM CFRP/GFRP rods," *Frattura ed Integrità Strutturale*, vol. 15, no. 58, pp. 386–401, Sep. 2021, https://doi.org/10.3221/IGF-ESIS.58.28.

[19] R. Devaraj, A. Olofinjana, and C. Gerber, "On the Factors That Determine the Bond Behaviour of GFRP Bars to Concrete: An Experimental Investigation," *Buildings*, vol. 13, no. 11, Nov. 2023, Art. no. 2896, https://doi.org/10.3390/buildings13112896.

[20] *Interim Testing Protocols for Determining the Seismic Performance Characteristics of Structural and Non-structural Components*, FEMA 461, Federal Emergency Management Agency Washington, D.C., Jun. 2007.